Packing Constraints and Electrostatic Surface Potentials Determine Transmembrane Asymmetry of Phosphatidylethanol

Alexander V. Victorov, Nathan Janes, Theodore F. Taraschi, and Jan B. Hoek
Department of Pathology, Anatomy, and Cell Biology, Thomas Jefferson University, Philadelphia, Pennsylvania 19107 USA

ABSTRACT The energetic determinants of the distribution of anionic phospholipids across a phosphatidylcholine (PtdCho) bilayer with different packing constraints in the two leaflets were studied, using $^{13}CH_2$-ethyl-labeled phosphatidylethanol (PtdEth) as a ^{13}C NMR membrane probe. PtdEth is unique in exhibiting a split $^{13}CH_2$-ethyl resonance in sonicated vesicles, the two components originating from the inner and outer leaflets, thus permitting the determination of the PtdEth concentration in each leaflet. Small and large unilamellar PtdEth-PtdCho vesicles were prepared in solutions of different ionic strengths. A quantitative expression for the transbilayer distribution of PtdEth, based on the balance between steric and electrostatic factors, was derived. The transbilayer difference in packing constraints was obtained from the magnitude of the PtdEth signal splitting. The electrostatic contribution could be satisfactorily described by the transmembrane difference in Gouy-Chapman surface potentials. At low (0.1–0.25%) PtdEth levels and high (up to 500 mM) salt concentrations, PtdEth had a marked fivefold preference for the inner leaflet, presumably because of its small headgroup, which favors tighter packing. At higher PtdEth content (4.8–9.1%) and low salt concentrations, where electrostatic repulsion becomes a dominant factor, the asymmetry was markedly reduced and an almost even distribution across the bilayer was obtained. In less curved, large vesicles, where packing constraints in the two leaflets are approximately the same, the PtdEth distribution was almost symmetrical. This study is the first quantitative analysis of the balance between steric and electrostatic factors that determines the equilibrium transbilayer distribution of charged membrane constituents.

INTRODUCTION

Many biological membranes are highly asymmetrical in the transbilayer distribution of phospholipids (Op den Kamp, 1979; Devaux, 1991). In the plasma membrane of mammalian cells, the zwitterionic phospholipids phosphatidylcholine (PtdCho) and sphingomyelin tend to be predominantly located in the exterior face. By contrast, phosphatidylethanolamine and phosphatidylserine, as well as negatively charged phospholipids, such as phosphatidic acid, phosphatidylglycerol, and phosphatidylinositol and its polyphosphoderivatives, are largely oriented toward the cytoplasm, where they participate in important physiological events, e.g., as precursors of second messengers or as regulatory elements for membrane-bound enzymes or vesicle trafficking (Nishizuka, 1992; Exton, 1994; Burgoyne, 1994; Liscovitch et al., 1994). The phospholipid asymmetry characteristic of a particular membrane is carefully maintained, and any changes in phospholipid distribution accompanying membrane assembly, synthesis, degradation, and intracellular trafficking are regulated by specialized enzymes (e.g., flippases) that catalyze transbilayer flow (Devaux, 1991; Menon, 1995). In the absence of flippase activity, however, the transbilayer movement of naturally occurring phospholipids is extremely slow, with a $t_{1/2}$ on the order of days (Barsukov et al., 1980; Menon, 1995), owing to the kinetic barrier in the hydrocarbon interior that prevents transmembrane diffusion of substances with highly polar or charged regions.

Even in artificial phospholipid vesicles, in the absence of flippase enzymes, anionic phospholipids often distribute asymmetrically (Michaelson et al., 1973; Berden et al., 1975; Barsukov et al., 1980; Nordlund et al., 1981; Pagano et al., 1981; Kumar and Gupta, 1984; Hope et al., 1989). The energetic basis of the uneven transmembrane distribution of these membrane constituents is poorly understood. A number of studies addressing the distribution of negatively charged phospholipids have pointed out the role of packing constraints and electrostatic repulsion (Israelachvili, 1973, 1991; McLaughlin and Harary, 1974; Berden et al., 1975; McQuarrie and Mulas, 1977; Low and Zilversmit, 1980; Barsukov et al., 1980; Tenchov and Koynova, 1985; Sundberg and Hubbell, 1986). However, none of these studies have considered the interplay between packing factors and electrostatic constraints in a quantitative framework.

Our interest in the energetic factors governing the transbilayer distribution and movement of anionic phospholipids was spurred by our observations of the unique membrane properties of phosphatidylethanol (PtdEth). PtdEth is an unusual anionic phospholipid formed in vivo in many cells and tissues in the presence of ethanol via a transphosphatidylation reaction catalyzed by phospholipase D (Alling et al., 1984; Gustavsson, 1995). PtdEth can accumulate to levels of up to 1–2% of total phospholipids in isolated cells treated with saturating concentrations of ethanol (>100 mM) and stimulated with an appropriate agonist (Moehren et al., 1994; Gustavsson, 1995). Local concentrations of

Received for publication 12 August 1996 and in final form 26 February 1997.

Address reprint requests to Dr. Jan B. Hoek, Department of Pathology, Anatomy and Cell Biology, Thomas Jefferson University, JAH 271, 1020 Locust Street, Philadelphia, PA 19107. Tel.: 215-503-5016; Fax: 215-923-2218; E-mail: hoek1@jeflin.tju.edu.

0006-3495/97/06/2588/11 $2.00

PtdEth may be even higher, whereas its degradation is relatively slow (Gustavsson, 1995). Very little is known about the biological consequences of PtdEth accumulation, although there have been reports that the activity of certain membrane-associated enzymes is affected by the presence of PtdEth (Asaoka et al., 1988; Omodeo-Sale et al., 1991). However, studies on artificial membrane systems demonstrated that PtdEth has unusual physicochemical properties that may be relevant for understanding its effects on biological membranes.

PtdEth possesses a small and relatively hydrophobic ethyl headgroup that endows it with unusual membrane properties (Browning, 1981; Omodeo-Sale et al., 1989). Among naturally occurring mammalian phospholipids, PtdEth exhibits a remarkable potency to impart a curvature stress upon the membrane bilayer (Lee et al., 1993, 1996). The alkyl headgroup of the phosphatidylalkanols tends to insert into the bilayer interior (Lee et al., 1996; Victorov et al., 1996). PtdEth undergoes unusually rapid transmembrane migration in unilamellar PtdCho vesicles, with a $t_{1/2}$ of less than 1 h (Victorov et al., 1994), i.e., one to two orders of magnitude faster than other mammalian phospholipids. Our initial observations demonstrated that this transbilayer movement of PtdEth could be induced by multivalent cations (Ca^{2+}, Pr^{3+}, Mn^{2+}) (Victorov et al., 1994). In more recent experiments, we found that electrostatic forces can trigger rapid transbilayer migration of PtdEth (Victorov et al., 1995, and unpublished data), indicating that PtdEth transfer occurs in the negatively charged form. This contrasts with previously reported mechanisms of transbilayer migration of phosphatidic acid and phosphatidylglycerol, which occurs in the electroneutral (protonated) form (Redelmeier et al., 1990; Eastman et al., 1991) and represents the first example of high rates of spontaneous flip-flop of a naturally occurring phospholipid in the anionic form. These observations raise the question of the factors governing the redistribution of PtdEth in the membrane.

In this paper we elucidate quantitatively the energetic principles governing the transbilayer distribution of negatively charged phospholipids using the PtdEth-PtdCho vesicle system in an equilibrated state, under different packing densities and electrostatic conditions. Small unilamellar vesicles (SUVs) were selected as a well-characterized model membrane system with intrinsically different packing constraints in the outer and inner monolayers. The transbilayer distribution of PtdEth can be readily obtained in this system from the ^{13}C-NMR spectra, in which the headgroup $^{13}CH_2$-ethyl resonance is split into two signals derived from labeled PtdEth molecules located in the inner and outer leaflets of the SUV (Victorov et al., 1994, 1996). Transbilayer differences in packing constraints and electrostatic surface potentials are obtained from the splitting of the PtdEth $^{13}CH_2$-ethyl resonance and from the distribution of the negatively charged phospholipids, respectively. The results demonstrate that these components satisfactorily account for the observed transbilayer distribution of PtdEth. The theoretical considerations derived here for PtdEth should apply equally to the transmembrane distribution of other negatively charged phospholipids in both stressed and unstressed bilayers.

MATERIALS AND METHODS

Reagents

Dioleoyl-PtdCho was purchased from Avanti Polar Lipids (Alabaster, AL). Labeled dioleoyl-PtdEth was synthesized as a sodium salt from dioleyl-PtdCho via a transphosphatidylation reaction catalyzed by peanut phospholipase D (EC 3.1.4.4; Sigma Chemical Co., St. Louis, MO), using [1-^{13}C]ethanol (99%; Cambridge Isotope Laboratories, Andover, MA) as described (Victorov et al., 1994). Unlabeled PtdEth was purchased from Avanti Polar Lipids. The purity of all lipids was greater than 99%, as determined by thin-layer chromatography using the solvent systems described previously (Moehren et al., 1994). Ethanol was obtained from Pharmco (Bayonne, NJ). All other reagents were obtained from Sigma.

Vesicle preparations

SUVs (40 mg/ml concentration of PtdCho, 5 mM Na acetate buffer with 25% ^2H_2O for ^2H lock, and KCl as noted) were prepared by ultrasonic irradiation of a handshaken lipid dispersion, purified by high-speed centrifugation and characterized as described in more detail elsewhere (Victorov et al., 1994, 1996). The pH was adjusted to 6.8 with a minimum of NaOH (<500 μM final concentration). Large unilamellar vesicles (LUVs) were prepared in the same buffer by an extrusion procedure using a double layer of polycarbonate filters (100-nm pore size) in a LipoFast extrusion apparatus (Avestin) (see Victorov et al., 1994).

NMR measurements

^{13}C-NMR noise-decoupled spectra were obtained on a Bruker AM 8.5T WB spectrometer operating at 90.6 MHz with a ^2H lock in a 10-mm probe without sample spinning, as described (Victorov et al., 1994). Typical conditions were 45° flip angle, 20.1-kHz broadband ^1H-decoupling power, 3.6-kHz broadband irradiation between acquisitions for NOE generation, 1.2 s between acquisitions, 20-kHz spectral window, 8 K data points zero-filled to 16 K, and 1-Hz exponential filtering, 3000–6000 transients. Saturation factors were determined for the inner and outer PtdEth $^{13}CH_2$-ethyl resonances at all extremes of composition (low and high salt, low and high PtdEth) and were equal. Thus the ratio of integral intensities of inner to outer PtdEth signals can be used to determine the transmembrane distribution of this phospholipid. Signal assignments were done as described earlier (Victorov et al., 1994, 1996). All measurements were taken at 295 ± 1 K.

Estimation of transbilayer phospholipid concentrations

The fractional populations of PtdCho and PtdEth in each leaflet were determined from the NMR spectra as described in detail previously (Victorov et al., 1994, 1996). Briefly, to obtain a precise estimate of the integral intensities of inner and outer $^{13}CH_2$-ethyl PtdEth signals, we carried out spectral simulations using a GRAMS/386 software package (NMR version). In some experiments, where peak splitting was small or where an unsplit $^{13}CH_2$-ethyl headgroup signal was observed, as in LUVs, the leaflet populations of PtdEth were determined after the addition of a low concentration (0.2–0.3 mM) of the shift reagent $Pr(NO_3)_3$ to the outer medium to separate the two components. This concentration was insufficient to induce a detectable transbilayer migration of PtdEth over the time course of these measurements. Similarly, quantitation of the leaflet populations of PtdCho was obtained using $Pr(NO_3)_3$ (8–10 mM) added to the outer medium of

SUVs or LUVs. The unshifted inner leaflet headgroup resonances of PtdCho ($N^+(CH_3)_3$, OCH_2, and N^+CH_2) were normalized to the acyl chain terminal methyl signal and compared to the corresponding total intensities before the addition of the shift reagent to yield the fraction of PtdCho in the inner leaflet, with the assumption that differences in T_1 and NOE for PtdCho in the inner and outer leaflets are small (Sears et al., 1976)

These measurements provide internal/external ratios of PtdCho and PtdEth, $\alpha = \text{PtdCho}^{in}/\text{PtdCho}^{out}$ and $\beta = \text{PtdEth}^{in}/\text{PtdEth}^{out}$. Because the total concentrations of PtdCho and PtdEth are known from the vesicle composition, the distribution of phospholipids between leaflets is obtained as follows:

$$\text{PtdCho}^{in} = \text{PtdCho}^{tot}/(\alpha^{-1} + 1)$$
$$\text{PtdCho}^{out} = \text{PtdCho}^{tot}/(\alpha + 1) \quad (1)$$

$$\text{PtdEth}^{in} = \text{PtdEth}^{tot}/(\beta^{-1} + 1)$$
$$\text{PtdEth}^{out} = \text{PtdEth}^{tot}/(\beta + 1) \quad (2)$$

The inner and outer mole fractions f_m^{in} and f_m^{out} of the individual phospholipids are calculated using the sum of all phospholipid populations in each leaflet:

$$\sum \text{PL}^{in} = \text{PtdCho}^{in} + \text{PtdEth}^{in} = \frac{\text{PtdCho}^{tot}}{\alpha^{-1} + 1} + \frac{\text{PtdEth}^{tot}}{\beta^{-1} + 1} \quad (3)$$

$$\sum \text{PL}^{out} = \text{PtdCho}^{out} + \text{PtdEth}^{out} = \frac{\text{PtdCho}^{tot}}{\alpha + 1} + \frac{\text{PtdEth}^{tot}}{\beta + 1} \quad (4)$$

Thus, for PtdEth,

$$f_m^{in} = \frac{\text{PtdEth}^{in}}{\sum \text{PL}^{in}} = \left\{1 + \frac{\text{PtdCho}^{tot}(\beta^{-1} + 1)}{\text{PtdEth}^{tot}(\alpha^{-1} + 1)}\right\}^{-1} \quad (5)$$

$$f_m^{out} = \frac{\text{PtdEth}^{out}}{\sum \text{PL}^{out}} = \left\{1 + \frac{\text{PtdCho}^{tot}(\beta + 1)}{\text{PtdEth}^{tot}(\alpha + 1)}\right\}^{-1} \quad (6)$$

Where surface concentrations were required in molecules per surface area (as in the estimation of surface charge densities), the phospholipid concentration in the inner or outer leaflets was divided by the phospholipid surface area, using estimates obtained from the literature (see Results).

THEORY

The distribution of a membrane-bound compound that equilibrates between the two leaflets of a bilayer can be described in terms of a partition coefficient, which we refer to as the coefficient of asymmetry (K_{as}). The free energy difference represented by the asymmetrical interleaflet equilibrium distribution (ΔG_{as}) provides a quantitative measure of the net energy required for the transfer of a molecule from one leaflet to the other. The relationship between ΔG_{as} and K_{as} is expressed by using the mole fraction f_m as the thermodynamically relevant concentration unit:

$$K_{as} = f_m^{in}/f_m^{out} = \exp(-\Delta G_{as}/RT) \quad (7)$$

Two energetic factors are considered to dominate ΔG_{as} for ionic species. One factor incorporates the different electrostatic forces across the bilayer ($\Delta\psi_{el}$); a second factor accounts for the difference in packing constraints between the two leaflets ($\Delta\mu_P$):

$$K_{as} = \exp(zF\Delta\psi_{el} + \Delta\mu_P)/RT \quad (8)$$

where z is the ionic charge, F is the Faraday constant, R is the gas constant, and T is the absolute temperature (295 K).

The electrostatic contribution ($\Delta\psi_{el}$) includes terms from both the surface electrostatic potential difference ($\Delta\psi_S$) and the Nernst transmembrane potential ($\Delta\psi_N$):

$$\Delta\psi_{el} = \Delta\psi_S + \Delta\psi_N \quad (9)$$

We assume that the Nernst transmembrane potential in the SUVs is negligible under the conditions used in these studies, where no further ion movements occurred after the equilibration of transmembrane potential differences during the sonication of the vesicles (see Results). The difference in surface electrostatic potentials between leaflets remains as the dominant electrostatic term.

$$\Delta\psi_S = (\psi_S)_{in} - (\psi_S)_{out} \quad (10)$$

Under conditions where PtdEth is the only charged species in the membrane, the surface charge density in each leaflet can be approximated from the PtdEth surface concentration (expressed in molecules/nm^2); the electrostatic surface potential can then be calculated using the Gouy-Chapman equation appropriate for the uni-univalent electrolytes used here, i.e., KCl, Na-acetate, and the sodium counterion of PtdEth (e.g., see McLaughlin et al., 1971; Cevc, 1990):

$$\sinh(zF\psi_S)/2RT = 1.36\sigma/C^{1/2} \quad (11)$$

The surface charge density in each leaflet, σ, is expressed in electronic charges per nm^2, C is the molar salt concentration, and ψ_S is the inner or outer surface potential.

The second energetic factor arises from the differences in packing constraints between the leaflets and produces a steric contribution ($\Delta\mu_P$) to the free energy difference. This, in turn, translates into a difference in mean phospholipid surface area between the inner and outer leaflets (which effectively reflects the difference in curvature energy between two monolayers). The steric contribution is isolated from the electrostatic contribution and determined experimentally under conditions where the electrostatic potential is negligible.

$$K_{as} = \exp(\Delta\mu_P^{(0)})/RT \quad (12)$$

where $\Delta\mu_P^{(o)}$ represents $\Delta\mu_P$ for $\psi_S \rightarrow 0$.

The electrostatic contribution becomes negligible when the surface charge density is small, which occurs at low PtdEth concentrations and high salt concentrations (see Results). Hence $\Delta\mu_P^{(o)}$ represents the distribution of very dilute PtdEth in an essentially pure PtdCho bilayer at high ionic strength.

A further energetic contribution is made by the interaction of electrostatic and packing factors that results in modulation of the phospholipid surface areas, e.g., by electro-

static expansion of the bilayer leaflets. Consequently, the packing density of the leaflets depends on the vesicle composition and ionic strength, and $\Delta\mu_P$ is not constant under all conditions investigated. To approximate the change in packing constraints that occurs with changes in surface charge density and ionic strength, we use information obtained from the splitting of the PtdEth [^{13}C]ethyl resonance, which reports on the interleaflet differences in packing density, as shown in previous studies (Victorov et al., 1994, 1996). $\Delta\mu_P$ is scaled linearly for the interleaflet difference in mean phospholipid surface area, ΔA, as determined from the chemical shift of the labeled PtdEth resonance and normalized to the mean transleaflet difference in phospholipid surface area in pure PtdCho vesicles, ΔA_o:

$$\Delta\mu_P = (\Delta A/\Delta A_0)\Delta\mu_P^{(0)} \quad (13)$$

Surface areas for PtdCho in the inner and outer leaflets of SUVs were obtained from the literature and assigned to the appropriate chemical shift of the labeled PtdEth resonance in vesicles of low PtdEth concentration and high ionic strength (see Results). Although the relationship between packing energy and phospholipid surface area may be more complex than the linear relationship shown, the equation accurately describes the extremes ($\Delta A = \Delta A_o$ when $\Delta\mu_P = \Delta\mu_P^{(o)}$; $\Delta A = 0$ when phospholipid surface areas are similar in either leaflet) and, therefore, provides an appropriate approximation over the limited range relevant for these estimates (e.g., Victorov et al., 1996, and further data in the Results section).

RESULTS

Experimental approach

Our previous studies (Victorov et al., 1994, 1996) demonstrated that the transbilayer distribution of low concentrations of PtdEth in SUVs is asymmetrical and can be modulated by changes in energetic driving forces exerted on one side of the bilayer. The relatively small headgroup and the conelike shape of the molecule promote its accommodation in the inner surface, where the packing constraints are tighter. We hypothesize that the packing forces that favor an inner leaflet orientation are opposed by surface electrostatic forces that tend to push more charged molecules to the outer surface. To quantitatively analyze the energetic contributions to PtdEth distribution, we used SUV preparations containing different PtdEth fractions and prepared at different ionic strengths, so as to vary the effective charge density at the membrane surface. The difference in surface electrostatic potentials is obtained from the surface concentration of PtdEth by Gouy-Chapman theory (Eq. 11). The transbilayer packing constraints inherent in the SUV preparations are estimated from K_{as} at dilute PtdEth levels (Eq. 12) and can be modulated independently by varying vesicle size. The transbilayer populations of PtdEth were monitored by NMR without further perturbation, avoiding complications related to transbilayer charge transfer or other changes in energy state.

Further information on vesicle characteristics is obtained from the ratio of the total to the inner signal for three major PtdCho headgroup resonances: $N^+(CH_3)_3$, OCH_2, and N^+CH_2, determined as described in Materials and Methods (spectra not shown). These ratios were not significantly different for preparations of SUVs containing up to 9% PtdEth. The total PtdCho/inner PtdCho ratios were 2.97 ± 0.05 (n = 3–4 for each PtdEth concentration), corresponding to outer PtdCho/inner PtdCho ratios of 1.97 ± 0.05. These ratios are in good agreement with the data reviewed by Hutton et al. (1977). Assuming a bilayer thickness λ = 4.0 nm and taking into account geometrical constraints based on a model of spherical vesicles with approximately similar molecular volumes of PtdCho in the internal and external leaflet (Huang and Mason, 1978), the observed PtdCho ratio is compatible with a mean surface area per phospholipid molecule, in the absence of PtdEth, of A^{in} = 0.57 nm^2 (inner leaflet) and A^{out} = 0.67 nm^2 (outer leaflet), in good agreement with literature data (Eisenberg and Chan, 1980; Sundberg and Hubbell, 1986; McIntosh et al., 1989; Nagle, 1993). These data correspond to vesicles with an outer diameter of 23.0–24.0 nm, containing 3900–4000 phospholipid molecules per vesicle, of which one-third are located in the inner leaflet and two-thirds are on the exterior surface. The difference in phospholipid surface area in the external and internal leaflets, ΔA_o, of ~0.10 nm^2 reflects the difference in packing density in these vesicles; this parameter is used to make adjustments for changes in packing energy under conditions of different PtdEth concentrations and ionic strengths, according to Eq. 13.

Transmembrane distribution of PtdEth in SUVs as a function of concentration and ionic strength

Representative examples of ^{13}C-NMR spectra of PtdCho-PtdEth SUVs are shown in Fig. 1. Vesicles were prepared with 1 mole% (Fig. 1 *A*) or 4.8 mole% (Fig. 1 *B*) of PtdEth in solutions of different concentrations of KCl (0–500 mM). The labeled resonance of PtdEth $^{13}CH_2$-ethyl is split into two components: a downfield peak, which corresponds to the outer leaflet population, and an upfield peak corresponding to the inner leaflet population. The resonances are readily distinguished from the (unsplit) resonances derived from PtdCho glycerol and OCH_2-choline (see also Victorov et al., 1996).

As shown in Figs. 1 and 2, the transbilayer distribution of PtdEth is highly asymmetrical at low concentrations of the phospholipid. However, the distribution depends on the PtdEth content of the vesicles and on the ionic strength of the solution. With increasing concentration of PtdEth, the electrostatic repulsion of negatively charged PtdEth molecules makes their inside accommodation energetically less favorable, and more PtdEth is found in the outer leaflet. The electrostatic effects of higher PtdEth levels are greatly re-

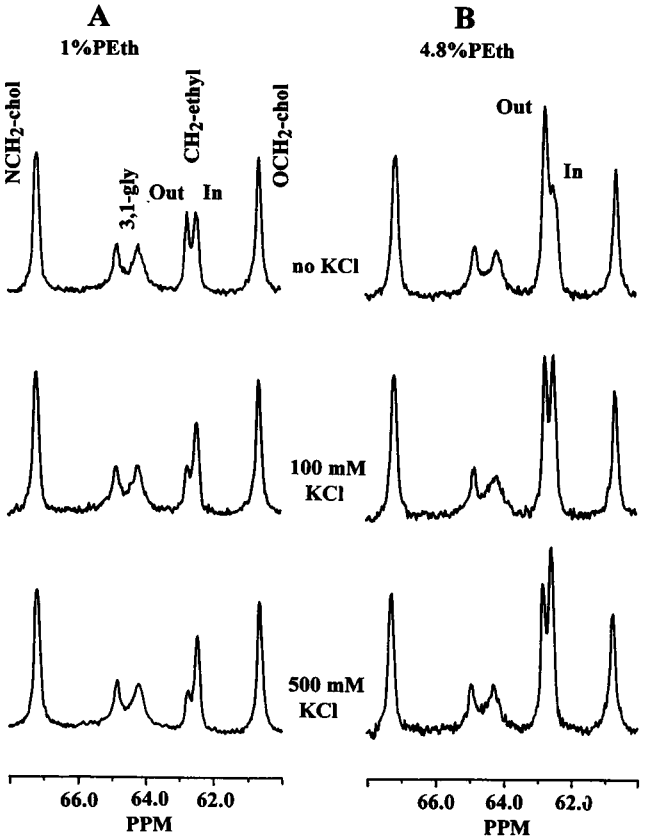

FIGURE 1 Effects of KCl concentration and PtdEth content on transbilayer distribution of PtdEth in PtdCho-PtdEth SUVs. (*A*) 1% ^{13}C-labeled PtdEth. (*B*) 4.8% PtdEth, containing 2% ^{13}C-labeled PtdEth. *Top spectra:* no KCl added; *middle spectra:* 100 mM KCl; *bottom spectra:* 500 mM KCl.

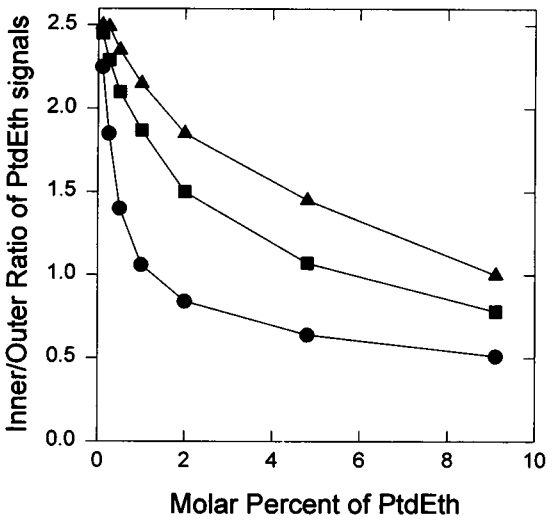

FIGURE 2 Experimentally measured integral intensity ratios of the inner/outer PtdEth signals in PtdCho-PtdEth SUVs at different KCl concentrations (relative error did not exceed 5%): no KCl (●); 100 mM KCl (■); 500 mM KCl (▲).

duced at high concentrations of KCl, and highly asymmetrical vesicles can be obtained, even at 9% PtdEth.

For a quantitative characterization of the transbilayer distribution of PtdEth in SUVs, which contain almost twice as many phospholipid molecules in the outer layer as in the inner leaflet, the ratio of surface mole fractions, f_m^{in}/f_m^{out}, is required rather than the integral intensities in each leaflet. Given the total amounts and relative proportions of PtdEth and PtdCho obtained from the NMR spectra, the transbilayer mole fractions of PtdEth are obtained as described in Materials and Methods (Eqs. 1–6). The calculated coefficients of asymmetry, K_{as}, are summarized in Table 1. These data clearly demonstrate the striking fivefold preference of PtdEth for the inner leaflet at low PtdEth levels, and the approach to a nearly equal distribution at high PtdEth levels.

Transbilayer packing constraints and surface charge density effects as a function of PtdEth concentration

Under conditions that minimize the effective net surface charge density (low PtdEth and high salt), K_{as} reaches a maximum value of 4.917 (Table 1). Because the acyl chains of both PtdEth and PtdCho species studied are homologous, the asymmetrical distribution reflects the small size of the PtdEth headgroup, which is more easily accommodated than PtdCho at the more densely packed inner surface. From the $K_{as}(\max) = 4.92$ observed at 0.1 mol % PtdEth and 0.5 M KCl, a difference of -3.91 kJ mol^{-1} in free energy of PtdEth packing in the unperturbed PtdCho matrix ($\Delta\mu_P^{(o)}$) is obtained according to Eq. 12 (see also Table 2).

An increase in PtdEth concentration in the SUVs not only affects the PtdEth distribution, but also the splitting between the outer and inner resonances. As shown in Table 2, as the concentration of PtdEth increases, both the inner and outer PtdEth signals move downfield, with the greater shift of the inner signal resulting in a decreased splitting between the inner and outer PtdEth signals, $\Delta\delta$. These findings indicate more equal packing constraints in the two monolayers at higher PtdEth levels, presumably reflecting the electrostatic expansion of the bilayer (Trauble, 1977). This, in turn, implies a larger mean area per phospholipid molecule, particularly in the inner monolayer. We have quantified changes in this parameter, using the dependencies of $\Delta\delta$ and the PtdEth peak chemical shift on PtdEth concentration (Table 2). The free energy difference of packing that is determined in the dilute limit at the plateau region ($\Delta\mu_P^{(o)}$) is scaled by the fractional decrease in areas, as shown in Eq. 13, to obtain $\Delta\mu_P$ at different PtdEth levels. In the absence of electrostatic expansion, i.e., at very low concentration of PtdEth, we assumed the difference between the mean phospholipid surface areas on the inner and outer leaflets ΔA to be minimal and equal to 0.10 nm^2 (Table 2). For calculations with higher concentrations of PtdEth, ΔA is estimated to decrease in proportion to the difference in chemical shift $\Delta\delta$ of the split PtdEth signal. Table 2 presents the chemical shifts, interleaflet packing energies, and surface packing

TABLE 1 Concentration and ionic strength dependencies of calculated coefficients of PtdEth transbilayer asymmetry in PtdCho-PtdEth SUVs

	No KCl			0.1 M KCl			0.5 M KCl		
Total PtdEth (mol%)	Inner PtdEth (mol%)	Outer PtdEth (mol%)	K_{as}	Inner PtdEth (mol%)	Outer PtdEth (mol%)	K_{as}	Inner PtdEth (mol%)	Outer PtdEth (mol%)	K_{as}
0.10	0.2054	0.0464	4.426	0.2107	0.0437	4.819	0.2119	0.0431	4.917
0.25	0.4809	0.1324	3.632	0.5155	0.1147	4.493	0.5283	0.1081	4.885
0.50	0.8631	0.3147	2.743	1.0009	0.2438	4.106	1.0361	0.2256	4.592
1.00	1.5203	0.7338	2.072	1.9173	0.5278	3.633	2.0066	0.4811	4.171
2.00	2.6926	1.6446	1.637	3.5092	1.2157	2.886	3.7856	1.0680	3.544
4.80	5.5212	4.4297	1.246	7.1846	3.5421	2.028	8.1413	3.0092	2.705
9.10	9.1259	9.0869	1.004	11.527	7.816	1.475	12.943	7.017	1.845

The mole fractions of PtdEth in the inner and outer leaflets were calculated by Eqs. 5 and 6, respectively, using the data of Fig. 2 for β values and a constant value for $\alpha = 1/1.97 = 0.5076$ (see text). The coefficient of PtdEth asymmetry was calculated as $K_{as} = f_m^{in}/f_m^{out}$.

density differences used in the calculations. The estimated changes in the mean phospholipid surface area are further used to calculate the net surface charge from PtdEth concentrations in inner and outer leaflets according to Eq. 11, as shown in Table 3.

Effect of the vesicle size on PtdEth distribution

The effect of transbilayer difference in packing constraints, $\Delta\mu_P$, on the distribution of PtdEth can be investigated by increasing vesicle size, as in LUVs. Under these conditions,

TABLE 2 NMR and packing constraint parameters for PtdCho-PtdEth SUVs

Total PtdEth (mol%)	δ_{out} (ppm)	δ_{in} (ppm)	$\Delta\delta$ (ppm)	A_{out} (nm^2)	A_{in} (nm^2)	ΔA (nm^2)	$\Delta\mu_P$ (kJ/mol)
				No KCl			
0.10	62.700	62.400	0.300	0.677	0.577	0.100	−3.91
0.25	62.700	62.410	0.290	0.677	0.580	0.097	−3.78
0.50	62.700	62.420	0.280	0.677	0.583	0.093	−3.65
1.00	62.700	62.430	0.270	0.677	0.587	0.090	−3.52
2.00	62.710	62.445	0.265	0.680	0.592	0.088	−3.45
4.80	62.730	62.520	0.210	0.687	0.617	0.070	−2.73
9.10	62.760	62.620	0.140	0.697	0.650	0.047	−1.82
				0.1 M KCl			
0.25	62.690	62.400	0.290	0.673	0.577	0.096	−3.78
0.50	62.690	62.400	0.290	0.673	0.577	0.096	−3.78
1.00	62.690	62.410	0.280	0.673	0.580	0.093	−3.65
2.00	62.700	62.420	0.280	0.677	0.583	0.094	−3.65
4.80	62.715	62.460	0.255	0.682	0.597	0.085	−3.32
9.10	62.750	62.560	0.190	0.693	0.630	0.063	−2.47
				0.5 M KCl			
0.25	62.680	62.380	0.300	0.670	0.570	0.100	−3.91
0.50	62.680	62.385	0.295	0.670	0.572	0.098	−3.84
1.00	62.685	62.390	0.295	0.672	0.573	0.098	−3.84
2.00	62.685	62.405	0.280	0.672	0.578	0.093	−3.65
4.80	62.695	62.435	0.260	0.675	0.588	0.087	−3.38
9.10	62.730	62.525	0.205	0.687	0.618	0.068	−2.67

$\Delta\delta$, the splitting between the outer (δ_{out}) and inner (δ_{in}) PtdEth signals; $\Delta\mu_P$, packing energy difference used in Eq. 8 and calculated through Eq. 13; ΔA, difference between areas per phospholipid molecule in the outer (A_{out}) and inner (A_{in}) leaflets of the SUV. These areas were calculated as follows: The smallest areas per phospholipid, $(A_{out})_{min} = 0.67$ nm^2 and $(A_{in})_{min} = 0.57$ nm^2 (giving a maximum $(\Delta A)_0 = 0.10$ nm^2), were assigned to the most tightly packed SUVs (0.1% PtdEth, 0.5 M KCl) characterized by the lowest chemical shifts for both the inner and outer PtdEth signals, $(\delta_{out})_{min} = 62.680$ ppm and $(\delta_{in})_{min} = 62.380$ ppm, and by the largest splitting $(\Delta\delta)_0 = 0.300$ ppm. The weighted molecular areas in other SUVs were calculated by proportional scaling, e.g., for the inner surface, A_{in} (nm^2) = $(A_{in})_{min} + (\Delta A)_0\{\delta_{in} - (\delta_{in})_{min}\}/\Delta\delta_0$. As PtdEth content is increased from 0.1 mol% to 9.1 mol%, the estimated area per phospholipid molecule steadily increases, which, in conjunction with the distribution of total phospholipids (obtained from the experimentally determined distribution ratios of PtdEth and PtdCho), was used to calculate the surface charge density in Eq. 11 (see Table 3). Relative error did not exceed 5%.

TABLE 3 Gouy-Chapman surface potentials for outer and inner leaflets of PtdCho-PtdEth SUVs prepared in solutions of different ionic strengths

	No KCl					0.1 M KCl			0.5 M KCl		
Mol% PtdEth	ψ_{out}	ψ_{in}	$\Delta\psi$ (mV)	ψ^*_{in}	$\Delta\psi^*$	ψ_{out}	ψ_{in} (mV)	$\Delta\psi$	ψ_{out}	ψ_{in} (mV)	$\Delta\psi$
0.10	−0.67	−3.46	−2.79	−4.15	−3.48	−0.14	−0.78	−0.64	−0.06	−0.36	−0.30
0.25	−1.88	−7.95	−6.07	−9.54	−7.66	−0.36	−1.90	−1.54	−0.16	−0.90	−0.74
0.50	−4.41	−13.87	−9.46	−16.64	−12.23	−0.77	−3.68	−2.91	−0.33	−1.75	−1.42
1.00	−9.94	−23.10	−13.15	−27.72	−17.78	−1.65	−6.95	−5.30	−0.69	−3.37	−2.68
2.00	−20.56	−36.54	−15.97	−43.84	−23.28	−3.74	−12.40	−8.66	−1.51	−6.22	−4.71
4.80	−44.87	−57.57	−12.70	−69.08	−24.21	−10.79	−24.26	−13.47	−4.29	−13.18	−8.89
9.10	−65.87	−69.12	−3.25	−82.94	−17.07	−22.71	−35.21	−12.50	−9.82	−19.74	−9.92

Values of ψ_{in} in the absence of KCl (marked with *) were increased by a factor of 1.20 to correct for the inner surface curvature effect (see text). The surface charge density in Eq. 11 was calculated from the experimentally measured PtdEth inner/outer signal intensity ratios (Fig. 2) and the constant PtdCho inner/outer signal intensity ratio $\alpha = 0.5076$, using estimated areas per phospholipid molecule in both leaflets obtained from Table 2.

the inner and outer PtdEth signals converge, with a chemical shift that is closer to the outer leaflet resonance of SUVs, and a shift reagent (e.g., Pr^{3+}) is required to differentiate between the leaflets. Because multivalent cations can induce PtdEth transbilayer movement (Victorov et al., 1994), we used a low concentration of Pr^{3+} (0.2–0.3 mM) sufficient to split the PtdEth signal, without affecting the initial distribution of PtdEth. As shown in Fig. 3, the PtdEth

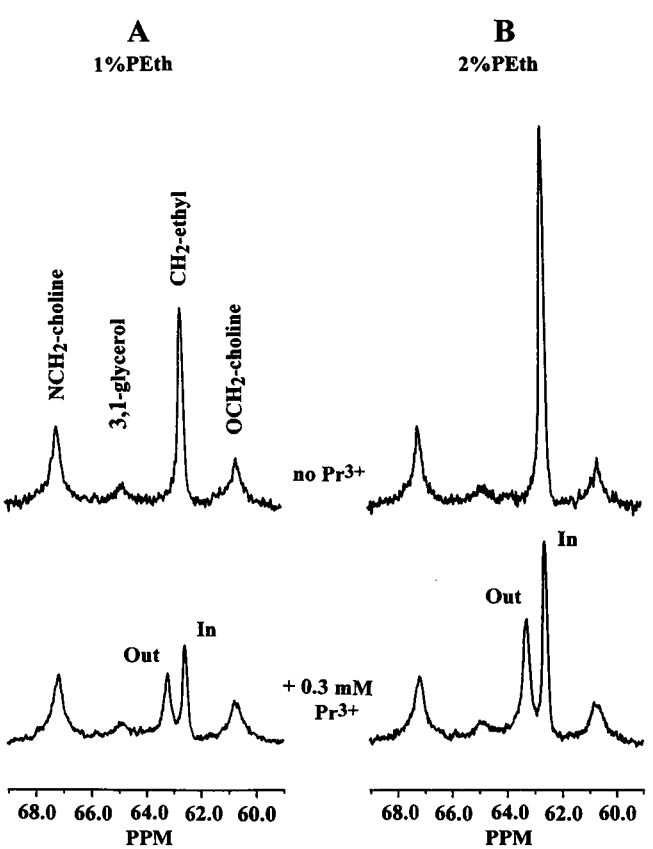

FIGURE 3 Transmembrane distribution of PtdEth in 100-nm LUVs prepared from PtdCho-1% ^{13}C-labeled PtdEth (no KCl present). (*A*) No Pr^{3+} added. (*B*) 0.3 mM Pr^{3+} added to the outer medium.

asymmetry in LUVs was substantially reduced compared to SUVs. The estimated K_{as} for 100-nm LUVs containing 1% PtdEth is approximately 1.2, compared to 2.1 for SUVs with the same concentration of PtdEth (no KCl). This distribution of PtdEth in LUVs corresponds to a difference in surface electrostatic potentials, $\Delta\psi_S$, of −3.5 mV. According to Eq. 8, the difference in packing energy in the two monolayers of the LUV, $\Delta\mu_P$, required to obtain the observed K_{as} of 1.2, would correspond to ~0.84 kJ/mol. Extrapolating from the data of Table 2, this difference in packing energy would correspond to a splitting between the inner and outer PtdEth signals, $\Delta\delta$, of about 0.06 ppm, well within the resolution limit of $\Delta\delta = 0.10–0.12$ ppm for PtdEth signals from the two leaflets, in agreement with the spectra shown in Fig. 3.

Energetics of the transbilayer distribution of PtdEth

Qualitatively, the transbilayer distribution of PtdEth fits the expectations of the energetic considerations outlined above. At low effective surface charge (low PtdEth, high salt), packing constraints are the dominant factor governing the distribution. PtdEth reaches a limiting preference for the inner leaflet that is attributed to the difference in headgroup size and packing abilities between PtdEth and PtdCho. At high effective surface charge (high PtdEth, low salt), electrostatics dominate the distribution. The initial interleaflet preference induced by packing constraints is countered by electrostatic demands that tend to equalize the surface potentials on each leaflet; consequently, the distribution approaches a value near unity.

A quantitative analysis of the energetics of the transbilayer distribution, K_{as}, based on Eqs. 7 and 8, employs the interleaflet packing free energy differences shown in Table 2 and the electrostatic surface potential differences obtained from Eq. 11 and summarized in Table 3. Equation 8 was rearranged in natural logarithmic form to compare the total estimated free energy difference $\Delta G_{as} = -(zF\Delta\psi_{el} + \Delta\mu_P)$

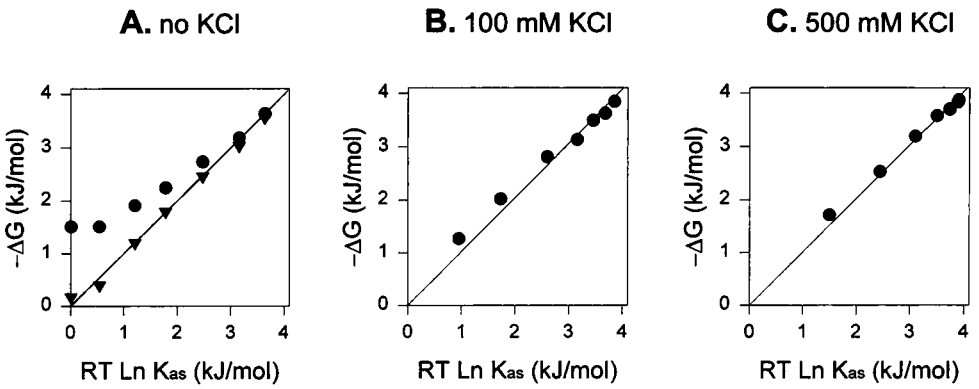

FIGURE 4 Logarithmic form of Eq. 8 showing the relationship between the K_{as} of PtdEth distribution (data from Table 1) and ΔG, estimated as the sum of electrostatic and packing energy differences across the bilayer (data from Tables 2 and 3). ▼, ΔG values calculated using the corrected ψ^*_{in} potentials; ●, uncorrected ΔG values. (*A*) No KCl added; (*B*) SUVs prepared in 100 mM KCl; (*C*) SUVs prepared in 500 mM KCl.

with the experimentally determined value of $RT \ln K_{as}$. The results are plotted in Fig. 4. Linear regression analysis indicates that at moderate and high salt concentrations (100 mM and 500 mM KCl), there is excellent quantitative agreement between the observed transbilayer distribution and the free energy changes determined from the surface potential and packing density differences, as predicted by the thermodynamic model (Fig. 4, *B* and *C*). However, at low ionic strengths (5 mM Na acetate and PtdEth counterions) the agreement is less satisfactory, particularly at modest to high PtdEth levels (Fig. 4 *A*), where the observed distribution corresponds to a greater electrostatic difference than modeled by the simple Gouy-Chapman analysis (Eq. 11).

Complications in the determination of the surface electrostatics in SUVs dispersed in low salt are well recognized. The difficulty has been attributed to relative sizes of the Debye length and the SUV inner diameter (Tenchov et al., 1984; Cevc, 1990). The electrostatic surface potential extending into the vesicle interior decays exponentially, but it can overlap portions of the inner leaflet that would be distant if the vesicle were not highly curved. The Debye length, the distance at which the surface potential is diminished by e times, equals 4.2, 1.0, and 0.3 nm for 5, 100, and 500 mM monovalent salt, respectively. This is to be compared with an inner radius of the SUVs of ~7.5–8.0 nm. Vesicles prepared in 100 or 500 mM KCl possess an inner surface potential, ψ_{in}, that does not exceed 35 mV (Table 3), the Debye length is small, and the simple Gouy-Chapman equation performs well without modification. In low salt solutions (5–10 mM Na^+), the Debye length becomes a significant fraction of the inner diameter and the surface potential is much larger and more sensitive to PtdEth content.

A number of workers have addressed the issue of electrostatic potentials of concave surfaces (e.g., Ohshima et al., 1982; Tenchov et al., 1984; Peitzsch et al., 1995). These studies indicated that exact general solutions are too complex to resolve. However, Tenchov et al. (1984) made numerical estimates of the electrostatic potentials inside small vesicles as a function of surface charge density, ionic strength, and the ratio of Debye length to vesicle radius. These findings indicate that the Gouy-Chapman surface potential calculated for planar surfaces may significantly underestimate the electrostatic potential of concave surfaces, particularly under low salt conditions. Using the theoretical curves reported by Tenchov et al. (1984), we estimate that in our experiments a correction factor of about 1.2 would be appropriate in the calculations of ψ_{in}. Consequently, the inner surface potentials under all conditions of low ionic strength were increased by 20% (Table 3). The corrected and uncorrected values are compared in Fig. 4 *A*. It is evident that this correction factor was sufficient to generate a satisfactory agreement between the observed K_{as} and the calculated value of ΔG. Although such a correction is an oversimplification, it does lend credence to the electrostatic origins of the deviation at low ionic strength, and thereby affirms the central point of this study: the distribution of PtdEth is determined by packing factors opposed by surface electrostatic factors.

DISCUSSION

Compared to other natural phospholipids, PtdEth is capable of relatively rapid diffusion across a lipid bilayer in both SUVs and LUVs in response to multicharged cations or electrostatic forces, with a $t_{1/2}$ on the order of 10–60 min (Victorov et al., 1994, 1995). However, this transbilayer migration is slow on the NMR time scale, and consequently, two distinct PtdEth signals from the inner and outer surfaces are observed in the ^{13}C-NMR spectra of SUVs containing this phospholipid. We made use of this characteristic of PtdEth to analyze the energetic factors (electrostatic and packing constraints) governing the distribution of PtdEth, using the relationship described in Eq. 8. Potentially, the same electrostatic or steric forces can, if unbalanced, drive PtdEth across the bilayer until a new equilibrium is reached. Similar energetic considerations would presumably apply to other anionic phospholipids. Previously, McLaughlin and Harary (1974) made an attempt to apply the Boltzmann equation to estimate the influence of electrostatic factors on the distribution of negatively charged phospholipids across the biological membranes. The expression of Eq. 8, used

here to characterize the transmembrane distribution of PtdEth, can similarly be regarded as describing a Boltzmann distribution. McLaughlin and Harary (1974) assumed that anionic phospholipids can freely travel between the two leaflets. However, it is now well documented that for nearly all naturally occurring negatively charged or zwitterionic phospholipids, this process of flip-flop is very slow, with a half-time of several days, because of the high activation energy of about 100 kJ/mol (Homan and Pownall, 1988).

In the experimental approach used here, equilibration of PtdEth distribution across the bilayer was obtained by exhaustive sonication of the vesicles under different conditions, thus enabling us to demonstrate that the equilibrium transbilayer distribution of PtdEth is sensitive to different energetic constraints in the membrane, as described by Eq. 8. The first term in Eq. 9 represents the electrostatic energy due to the difference in Gouy-Chapman surface potentials, $\Delta\psi_S$, which, owing to the predominant location of PtdEth in the inner leaflet, is negative inside. The electrostatic energy for accommodation of PtdEth in the inner monolayer is higher than that for the outer leaflet and, hence, the difference $zF\Delta\psi_S$ is positive. Thus $\Delta\psi_S$ can serve as a potential driving force for outward movement of negatively charged PtdEth. A second electrostatic term in Eq. 9 would ensue from a Nernst transmembrane potential, $\Delta\psi_N$. Under conditions used here, where no charge transfer occurs across the bilayer after exhaustive sonication of the vesicles, we assume $\Delta\psi_N = 0$. In addition to the electrostatic terms, we introduce a steric factor, $\Delta\mu_P$, the difference in chemical potential of PtdEth in the inner and outer leaflets, which reflects a transmembrane difference in packing density. Because steric constraints in the inner leaflet favor the accommodation of PtdEth, the difference in packing energy, $\Delta\mu_P$, is negative. In SUVs, $\Delta\mu_P$ represents the effect of bilayer curvature on the distribution of the charged PtdEth, but, in principle, $\Delta\mu_P$ can be used to describe differences in chemical potential due to steric constraints, even in a planar bilayer with different packing conditions in each leaflet. The contribution of steric factors to the asymmetrical distribution of PtdEth, represented by the transmembrane chemical potential difference $\Delta\mu_P$, varied in the range from -3.9 to -1.8 kJ/mol for different SUVs (Table 2).

It should be pointed out that the asymmetrical distribution of PtdEth does not reflect a differential protonation due to a pH gradient across the vesicle membrane. The apparent pK_a of PtdEth for both the inner and outer surfaces of the SUVs is <4, as was earlier determined from the pH dependence of the chemical shift of the inner and outer $[^{13}C]H_2$-ethyl signals, with the apparent pK_a on the inner surface being 0.6–0.8 pH units higher than in the outer leaflet (Victorov et al., 1996). No protonation of PtdEth or changes in its transmembrane distribution were detectable in the SUVs at pH 6.5–7.5 at the PtdEth concentrations used in the present experiments.

The satisfactory agreement found between the experimentally observed K_{as} and theoretical free energy changes estimated from the electrostatic ($zF\Delta\psi_S$) and packing ($\Delta\mu_P$) energy terms (Eq. 8, Fig. 4) supports our three main assumptions: 1) the equilibrium transmembrane distribution of PtdEth can be described adequately by a partition coefficient; 2) the difference in electrostatic energy between two monolayers can be calculated using the Gouy-Chapman equation (provided appropriate corrections for the small vesicle diameters relative to the Debye length are introduced); and 3) the splitting of the $[^{13}C]H_2$-ethyl PtdEth signal is proportional to the difference in packing energy for PtdEth molecules in the two leaflets.

Our present experimental data refer mainly to the distribution of PtdEth in small phospholipid vesicles. However, the same approach can be used to describe the distribution of other negatively charged phospholipids in model membranes, given that the transbilayer gradient of packing constraints is reliably measured or calculated. Although biological membranes generally are less curved than those of SUVs, the two leaflets of the same bilayer frequently possess different packing conditions because of asymmetrical distribution of membrane constituents that influence this property (e.g., cholesterol, specific phospholipid species, integral membrane proteins). In this case, Eq. 8 describes the transmembrane equilibrium distribution of charged species that diffuse across the bilayer. These could include lipids such as PtdEth, lipophilic drugs, and various distributional membrane probes (e.g. tetraphenylboron or tetraphenylphosphonium; Flewelling and Hubbell, 1986).

In summary, the experimental data reported here demonstrate that PtdEth possesses unique membrane properties that reflect the high sensitivity of this phospholipid to its environment. The main objective of this investigation was to elucidate and quantify the factors that determine the transbilayer distribution of PtdEth as an anionic phospholipid. The data show that the equilibrium distribution of PtdEth across the lipid bilayer is governed by transmembrane differences in both electrostatic surface potentials and packing constraints. These same factors should be taken into account as potential driving forces for transmembrane movement of this lipid reported earlier (Victorov et al., 1994, 1995).

The extent to which these factors also influence the distribution of PtdEth generated in biological membranes remains to be investigated. In intact cells, nonequilibrium distributions of phospholipids are often maintained by enzymes that catalyze transbilayer migration, such as flippases (Devaux, 1991). The activity of these enzymes with respect to an unusual phospholipid molecule, such as PtdEth, is not known. The physiological role of phospholipase D, the enzyme that generates phosphatidic acid or PtdEth, has not yet been adequately identified. However, recent studies suggested a function of the enzyme in membrane fusion events, a process that involves transient conditions of high membrane curvature (Cockcroft et al., 1994; Liscovitch, 1994). Thus a local accumulation of phosphatidic acid or PtdEth in these areas may have functional implications.

This work was supported by U.S. Public Health Service grants AA07186, AA07215, AA00163, and AA08714.

REFERENCES

Alling, C., L. Gustavsson, J.-E. Mansson, G. Benthin, and E. Anggard. 1984. Phosphatidylethanol formation in rat organs after ethanol treatment. *Biochim. Biophys. Acta.* 793:119–122.

Asaoka, Y., U. Kikkawa, K. Sekiguchi, M. S. Shearman, Y. Kosaka, Y. Nakano, T. Satoh, and Y. Nishizuka. 1988. Activation of a brain-specific protein kinase C subspecies in the presence of phosphatidylethanol. *FEBS Lett.* 231:221–224.

Barsukov, L. I., A. V. Victorov, I. A. Vasilenko, R. P. Evstigneeva, and L. D. Bergelson. 1980. Investigation of the inside-outside distribution, intermembrane exchange and transbilayer movement of phospholipids in sonicated vesicles by shift reagent NMR. *Biochim. Biophys. Acta.* 598: 153–168.

Berden, J. A., R. W. Barker, and G. K. Radda. 1975. NMR studies on phospholipid bilayers. Some factors affecting lipid distribution. *Biochim. Biophys. Acta.* 375:186–208.

Browning, J. L. 1981. Motions and interactions of phospholipid head groups at the membrane surface. Simple alkyl head groups. *Biochemistry.* 20:7123–7133.

Burgoyne, R. 1994. Phosphoinositides in vesicular traffic. *Trends Biochem. Sci.* 19:55–57.

Cevc, G. 1990. Membrane electrostatics. *Biochim. Biophys. Acta.* 1031: 311–382.

Cockcroft, S., G. M. H. Thomas, A. Fensome, B. Geny, E. Cunningham, I. Gout, I. Hiles, N. F. Totty, O. Truong, and J. J. Hsuan. 1994. Phospholipase D: a downstream effector of ARF in granulocytes. *Science.* 263:523–526.

Devaux, P. F. 1991. Static and dynamic lipid asymmetry in cell membranes. *Biochemistry.* 30:1163–1173.

Eastman, S. J., M. J. Hope, and P. R. Cullis. 1991. Transbilayer transport of phosphatidic acid in response to transmembrane pH gradients. *Biochemistry.* 30:1740–1745.

Eisenberg, K. E., and S. I. Chan. 1980. The effects of surface curvature on the headgroup structure and phase transition properties of phospholipid bilayer vesicles. *Biochim. Biophys. Acta.* 599:330–335.

Exton, J. H. 1994. Phosphatidylcholine breakdown and signal transduction. *Biochim. Biophys. Acta.* 1212:26–42.

Flewelling, R. F., and W. L. Hubbell. 1986. The membrane dipole potential in a total membrane potential model. Applications to hydrophobic ion interactions with membranes. *Biophys. J.* 49:541–551.

Gustavsson, L. 1995. Phosphatidylethanol formation-specific effects of ethanol mediated via phospholipase D. *Alcohol Alcohol.* 30:391–406.

Homan, R., and H. J. Pownall. 1988. Transbilayer diffusion of phospholipids: dependence on headgroup structure and acyl chain length. *Biochim. Biophys. Acta.* 938:155–166.

Hope, M. J., T. E. Redelmeier, K. F. Wong, W. Rodrigueza, and P. R. Cullis. 1989. Phospholipid asymmetry in large unilamellar vesicles induced by transmembrane pH gradients. *Biochemistry.* 28:4181–4187.

Huang, C., and J. T. Mason. 1978. Geometric packing constraints in egg phosphatidylcholine vesicles. *Proc. Natl. Acad. Sci. USA.* 75:308–310.

Hutton, W. C., P. L. Yeagle, and R. B. Martin. 1977. The interaction of lanthanide and calcium salts with phospholipid bilayer vesicles: the validity of the nuclear magnetic resonance method for determination of vesicle bilayer phospholipid surface ratios. *Chem. Phys. Lipids.* 19: 255–265.

Israelachvili, J. N. 1973. Theoretical considerations on the asymmetric distribution of charged phospholipid molecules on the inner and outer layers of curved bilayer membranes. *Biochim. Biophys. Acta.* 323: 659–663.

Israelachvili, J. N. 1991. Intermolecular and Surface Forces. Academic Press, New York.

Kumar, A., and C. M. Gupta. 1984. Transbilayer distributions of red cell membrane phospholipids in unilamellar vesicles. *Biochim. Biophys. Acta.* 769:419–428.

Lee, Y.-C., T. F. Taraschi, and N. Janes. 1993. Support for the shape concept of lipid structure based on a headgroup volume approach. *Biophys. J.* 65:1429–1432.

Lee, Y.-C., Y. O. Zheng, T. F. Taraschi, and N. Janes. 1996. Hydrophobic alkyl headgroups strongly promote membrane curvature and violate the headgroup volume correlation due to headgroup insertion. *Biochemistry.* 35:3677–3684.

Liscovitch, M., V. Chalifa, P. Pertile, C. S. Chen, and L. C. Cantley. 1994. Novel function of phosphatidylinositol 4,5-bisphosphate as a cofactor for brain membrane phospholipase D. *J. Biol. Chem.* 269: 21403–21406.

Low, M. G., and D. B. Zilversmit. 1980. Phosphatidylinositol distribution and translocation in sonicated vesicles. A study with exchange protein and phospholipase C. *Biochim. Biophys. Acta.* 596:223–234.

McIntosh, T. J., A. D. Magid, and A. Simon. 1989. Range of the solvation pressure between lipid membranes: dependence on the packing density. *Biochemistry.* 28:7904–7912.

McLaughlin, S., and H. Harary. 1974. Phospholipid flip-flop and the distribution of surface charges in excitable membranes. *Biophys. J.* 14:200–208.

McLaughlin, S. G. A., G. Szabo, and G. Eisenman. 1971. Divalent cations and the surface potential of charged phospholipid membranes. *J. Gen. Physiol.* 58:667–687.

McQuarrie, D. A., and P. Mulas. 1977. Asymmetric charge distributions in planar bilayer systems. *Biophys. J.* 17:103–109.

Menon, A. K. 1995. Flippases. *Trends Cell Biol.* 5:355–360.

Michaelson, D. M., A. F. Horwitz, and M. P. Klein. 1973. Transbilayer asymmetry and surface homogeneity of mixed phospholipids in cosonicated vesicles. *Biochemistry.* 12:2637–2645.

Moehren, G., L. Gustavsson, and J. B. Hoek. 1994. Activation and desensitization of phospholipase D in intact rat hepatocytes. *J. Biol. Chem.* 269:838–848.

Nagle, J. F. 1993. Area/lipid of bilayers from NMR. *Biophys. J.* 64: 1476–1481.

Nishizuka, Y. 1992. Intracellular signaling by hydrolysis of phospholipids and activation of protein kinase C. *Science.* 258:607–614.

Nordlund, J. R., C. F. Schmidt, S. N. Dicken, and T. E. Thompson. 1981. Transbilayer distribution of phosphatidylethanolamine in large and small unilamellar vesicles. *Biochemistry.* 20:3237–3241.

Ohshima, H., T. W. Healy, and L. R. White. 1982. Accurate analytic expressions for the surface charge density/surface potential relationship and double layer potential distribution for a spherical colloidal particle. *J. Colloid Interface Sci.* 90:17–26.

Omodeo-Sale, F., B. Cestaro, A. Mascherpa, D. Monti, and M. Masserini. 1989. Enzymatic synthesis and thermotropic behaviour of phosphatidylethanol. *Chem. Phys. Lipids.* 50:135–142.

Omodeo-Sale, F., C. Lindi, P. Palestini, and M. Masserini. 1991. Role of phosphatidylethanol in membranes. Effects on membrane fluidity, tolerance to ethanol, and activity of membrane-bound enzymes. *Biochemistry.* 30:2477–2482.

Op den Kamp, J. 1979. Lipid asymmetry in membranes. *Annu. Rev. Biochem.* 48:47–71.

Pagano, R. E., O. C. Martin, A. J. Schroit, and D. K. Struck. 1981. Formation of asymmetric phospholipid membranes via spontaneous transfer of fluorescent lipid analogues between vesicle populations. *Biochemistry.* 20:4920–4927.

Peitzsch, R. M., M. Eisenberg, K. A. Sharp, and S. McLaughlin. 1995. Calculations of the electrostatic potential adjacent to model phospholipid bilayers. *Biophys. J.* 68:729–738.

Redelmeier, T. E., M. J. Hope, and P. R. Cullis. 1990. On the mechanism of transbilayer transport of phosphatidylglycerol in response to transmembrane pH gradients. *Biochemistry.* 29:3046–3053.

Sears, B., W. C. Hutton, and T. E. Thompson. 1976. Effects of paramagnetic shift reagents on the ^{13}C nuclear magnetic resonance spectra of egg phosphatidylcholine enriched with ^{13}C in the N-methyl carbons. *Biochemistry.* 15:1635–1639.

Sundberg, S. A., and W. L. Hubbell. 1986. Investigation of surface potential asymmetry in phospholipid vesicles by a spin label relaxation method. *Biophys. J.* 49:553–562.

Tenchov, B. G., and R. D. Koynova. 1985. The effect of nonideal lateral mixing on the transmembrane lipid asymmetry. *Biochim. Biophys. Acta.* 815:380–391.

Tenchov, B. G., R. D. Koynova, and B. D. Raytchev. 1984. The electric double layer inside a sherical aqueous cavity: a comparison between exact numerical and approximate analytical solutions. *J. Colloid Interface Sci.* 102:337–347.

Trauble, H. 1977. Membrane electrostatics. *In* Structure and Function of Biological Membranes. Plenum, New York. 509–550.

Victorov, A. V., N. Janes, G. Moehren, E. Rubin, T. F. Taraschi, and J. B. Hoek. 1994. Rapid transbilayer movement of phosphatidyethanol in unilamellar phosphatidylcholine vesicles. *J. Am. Chem. Soc.* 116: 4050–4052.

Victorov, A. V., N. Janes, G. Moehren, E. Rubin, T. F. Taraschi, and J. B. Hoek. 1995. Rapid transbilayer migration of phosphatidylethanol in liposomes is determined by transbilayer electrostatics and packing constraints. *Alcohol. Clin. Exp. Res.* 19(2):59A. (Abstr.)

Victorov, A. V., T. F. Taraschi, and J. B. Hoek. 1996. Phosphatidylethanol as a ^{13}C NMR probe for reporting packing constraints in phospholipid membranes. *Biochim. Biophys. Acta.* 1283:151–162.